Brazilian Journal
of Chemical
Engineering

ISSN 0104-6632
Printed in Brazil
www.scielo.br/bjce

Vol. 35, No. 01, pp. 155 – 167, January – March, 2018
dx.doi.org/10.1590/0104-6632.20180351s20160299

EFFECT OF LIME ADDITION TO $CASO_4$ OXYGEN CARRIER IN CHEMICAL LOOPING COMBUSTION

Ning Ding[1,2*], Pengfei Zhang[1,3], Ning Guan[1], Guilin Jiang[1],
Chengwu Zhang[1] and Zhigang Liu[1*]

[1] Key laboratory for Flow & Enhanced Heat Transfer of Shandong Academy of Sciences, Jinan, 250014, China
[2] HEBEI Ji-Yan Energy Science and Technology Research Institute CO., LTD, Shijiazhuang, 050000, China
[3] School of Energy Power and Mechanical Engineering, North China Electric Power University, Baoding, 071003, China

(Submitted: May 5, 2016; Revised: September 19, 2016; Accepted: November 1, 2016)

Abstract – Chemical-looping combustion (CLC), which has the characteristic of greenhouse gas CO_2 inherent separation, is a novel combustion technology. In this study, CLC experiments of methane using $CaSO_4$ oxygen carrier with lime addition were carried out in a batched fluidized bed reactor, where the sample was exposed to alternate oxidizing and reducing conditions. The influences of temperature, calcium-to-sulphur ratio and lime particle size on the conversion of $CaSO_4$ and sulfur capture were investigated and a suitable operation condition was determined. Under the optimal operation condition, a multi-cycle test was performed to evaluate the cyclic redox behavior of the lime-promoted $CaSO_4$ sample. X-ray diffraction and a field emission scanning electron microscope were used to characterize the phase and surface morphology of the samples used. The results show that the addition of lime could improve the conversion rate of $CaSO_4$ and the capture efficiency of sulfur-containing gases. The operation conditions of calcium-to-sulfur ratio 0.8, lime particle size of 180-250 μm and operation temperature of 900 °C turned out to be the optimal conditions. Besides, the average desulphurization rate of lime was up to 78.77% during the cyclic test.

Keywords: Chemical-looping combustion; lime; CaSO4; sulfur capture.

INTRODUCTION

It is well known that fossil fuel consumption is the major source of anthropogenic CO_2 emission. There are numerous techniques that can potentially be used for CO_2 separation and compression from combustion, but most of them are considered to be energy intensive (Stern and Hatton, 2014; Liu et al., 2005; Notz et al., 2007). Chemical-looping combustion (CLC) is a novel combustion technology where CO_2 is separated from the flue gases without such an energy-consuming gas separation process. (Ding et al., 2015; Abad et al., 2006; Johansson et al., 2006; Adánez et al., 2009).

CLC involves the use of oxygen carrier, which transfers oxygen from air to allow fuel oxidation, thus avoiding the direct contact between fuel and air. Typically, a dual fluidized bed system composed of an air reactor (AR) and a fuel reactor (FR) is widely applied in CLC process (Ding et al., 2012). In the FR, fuel (natural gas, refinery gas, synthesis gas from coal gasification, etc.) is oxidized via an oxygen carrier to produce CO_2 and steam. After a steam condensation process, high-purity CO_2 can be easily obtained without extra energy consumption. The reduced oxygen carrier is further transferred to the AR where it is re-oxidized by air. Since this is an exothermic reaction, the temperature of gases consisting of N_2 and residual O_2 increases substantially. After that, the oxygen carrier with high oxygen potential is recirculated to the FR for a new cycle. The reduction reaction is either endothermic or slightly exothermic depending on the kinds of the oxygen carrier and the fuel. The total amount of heat evolved from the two reactions is equivalent to that of normal combustion

* *Corresponding author.* Ning Ding. E-mail: 864911600@163.com; Zhigang Liu. E-mail: zgliu9322@163.com; Phone: +86-531-85599030. Fax: +86-531-82961954

of the same fuel (Cao and Pan, 2006; Scott et al., 2006; de Diego et al., 2008).

$CaSO_4$, as a low cost potential oxygen carrier for CLC, has attracted increasing attention all over the world recently. ALSTOM Power Co. Ltd. (Andrus et al., 2009) studied the limestone-based chemical looping process, and a plant facility at a power scale of 3 MW_{th} using $CaSO_4$ as the oxygen carrier has been constructed and operated. Shen and Xiao at the Southeast University in China also investigated the feasibility of $CaSO_4$ as an oxygen carrier (Shen et al., 2008; Song et al., 2008a), reactivity test with gaseous and solid fuels (Zheng et al., 2010; Song et al., 2008b), and the reduction kinetics (Zheng et al., 2011; Xiao et al., 2011). The results demonstrated that $CaSO_4$ was an alternative oxygen carrier with high oxygen capacity. However, it has been verified that the potential sulfur release results in a decline in the reactivity of $CaSO_4$ during the reduction/oxidation process. Thus, the sulfur release is a major challenge for the practical application of $CaSO_4$ oxygen carrier.

For $CaSO_4$/CaS oxygen carrier, the main reactions occuring in the FR and AR with methane as fuel are shown as follows:

$$CaSO_4 + CH_4 \rightarrow CaS + CO_2 + 2H_2O \ \Delta H^0_{298K} = 159.6 \text{ kJ/mol} \quad \text{(R1)}$$

$$CaS + 2O_2 \rightarrow CaSO_4 \Delta H^0_{298K} = -962.4 \text{ kJ/mol} \quad \text{(R2)}$$

As illustrated in many previous investigations (Anthony and Granatstein, 2001; Mattisson and Lyngfelt, 1998; Tian et al., 2010; Ding et al., 2011), the emission of sulfur related to $CaSO_4$ and CaS varied with the operating conditions. In this paper, SO_2 and H_2S are mainly formed from the following side reactions during the reduction (R3, R4, R5) and oxidation (R5, R6).

$$CaSO_4 + CH_4 \rightarrow CaO + CO_2 + H_2O + H_2S \ \Delta H^0_{298K} = 221.17 \text{ kJ/mol} \quad \text{(R3)}$$

$$4CaSO_4 + CH_4 \rightarrow 4CaO + CO_2 + 2H_2O + 4SO_2 \Delta H^0_{298K} = 1220.80 \text{ kJ/mol} \quad \text{(R4)}$$

$$3CaSO_4 + CaS \rightarrow 4CaO + 4SO_2 \Delta H^0_{298K} = 1061.34 \text{ kJ/mol} \quad \text{(R5)}$$

$$CaS + 3/2O_2 \rightarrow CaO + SO_2 \Delta H^0_{298K} = -456.73 \text{ kJ/mol} \quad \text{(R6)}$$

The sulfur release will lead to atmospheric pollution, and decrease the oxygen transfer capacity of $CaSO_4$ oxygen carrier. Therefore, it is necessary to reduce the sulfur release in the CLC of $CaSO_4$ oxygen carrier. Limestone ($CaCO_3$) particles are widely used in circulating fluidized beds for sulfur capture (Saastamoinen and Shimizu, 2007; Bragança et al., 2003,2009; Sebag et al., 2001). The addition of limestone sorbent may be a reasonable method to capture sulfur and decrease the sulfur release during the reduction/oxidation process (Song et al., 2008b). If the fresh limestone particles are fed into the FR, $CaCO_3$ can be converted to CaO (R7) depending on the partial pressure of CO_2. Therefore, after CaO or $CaCO_3$ addition, the following reactions may take place in the reactors:

$$CaCO_3 \rightarrow CaO + CO_2 \Delta H^0_{298K} = 178.16 \text{ kJ/mol} \quad \text{(R7)}$$

$$CaO + H_2S \rightarrow CaS + H_2O \ \Delta H^0_{298K} = -61.40 \text{ kJ/mol} \quad \text{(R8)}$$

$$CaO + SO_2 \rightarrow CaSO_3 \Delta H^0_{298K} = -227.65 \text{ kJ/mol} \quad \text{(R9)}$$

$$CaO + 3CO + SO_2 \rightarrow CaS + 3CO_2 \Delta H^0_{298K} = -392.16 \text{ kJ/mol} \quad \text{(R10)}$$

$$CaCO_3 + H_2S \rightarrow CaS + H_2O + CO_2 \Delta H^0_{298K} = 72.77 \text{ kJ/mol} \quad \text{(R11)}$$

The oxygen carrier particles, desulphurization products (CaS and $CaSO_3$), and residual CaO are all transferred into AR and these bed materials can be oxidized to $CaSO_4$ in the oxidation condition. Besides, the SO_2 released in the AR may also be captured by CaO:

$$CaO+SO_2+1/2O_2 \rightarrow CaSO_4 \Delta H^0_{298K} = -505.89 \text{ kJ/mol} \quad \text{(R12)}$$

In other ways, the sulfur-containing gases released in the process of the fuel conversion, i.e., H_2S and SO_2, may have a positive effect on fuel gasification in CLC of solid fuel (Mattisson and Lyngfelt, 1999; Lyon and Cole, 2000). The influence of lime and limestone addition to ilmenite oxygen carrier was investigated in a laboratory-batched fluidized bed reactor (Teyssié et al., 2011) and in a continuous 10 kW_{th} CLC pilot reactor with solid fuel (Cuadrat et al., 2011), respectively. The addition of CaO to ilmenite improved the gas conversion, which can be explained by the catalytic effect of CaO on the conversion of CO to H_2 (by the water-gas shift reaction) and the high reactivity of ilmenite oxygen carrier toward H_2.

In this study, thermodynamics and kinetics of $CaSO_4$ oxygen carrier with lime addition in CLC of methane was discussed. To be more specific, the effects of temperature, calcium to sulphur ratio and lime particle size on conversion of $CaSO_4$ and sulfur capture were analyzed. Moreover, the used oxygen carriers were also characterized through X-ray diffraction (XRD) analysis and field emission scanning electron microscope (FESEM).

EXPERIMENTAL SECTION

Material

The oxygen carrier particle used in the present study was originated from the natural anhydrite ore (provided by the Wanbei Coal-Electricity Group CO., LTD), which was further crushed by pulverizer and sieved to a size range of 180-250 μm. The natural anhydrite ore is composed of $CaSO_4$ and a small proportion of other impurity, as presented in Table 1. The apparent density and bulk density of the particles are 2950 and 1510 kg/m^3, respectively.

As the main components of the limestone, $CaCO_3$ accounts for a mass fraction of 95.67 % and the other components are MgO (1.75 wt.%), SiO_2 (1.26 wt.%), Al_2O_3 (0.82 wt.%), and Fe_2O_3 (0.50 wt.%). In a previous sulfur capture process, the optimum calcinations temperature was found to be 950 °C (Doğu, 1981). Therefore, the limestone was fully calcined in a fixed bed with an inert gas flow of nitrogen at 950 °C until the CO_2 disappeared in the exhaust gas, and the lime obtained was used in the CLC experiments. The composition of the samples used was determined by XRD test using Cu-Kα radiation over a 2θ range of 15-85°. The surface morphology of samples was measured by FESEM (Sirion 200, Holland).

Table 1. Composition of natural anhydrite (wt.%).

Chemical composition	Value
$CaSO_4$	95.02
CaO	1.25
SiO_2	0.65
MgO	0.46
Al_2O_3	0.25
TiO_2	0.05
Fe_2O_3	0.02
Crystallization water	2.30

Experimental Setup

Figure 1 shows the experimental apparatus used for testing the oxygen carriers. It consisted of a gas feed, a fluidized reactor, a tube furnace, a cooler and a gas analysis system. A porous distributor plate was located in the middle stainless-steel tube (I.D. =40 mm, length =900 mm). The reactor was heated in an electric furnace, and the furnace temperature was controlled by a K-type thermocouple between the reactor tube and the heater, while the temperature was also monitored by another K-type thermocouple inside the oxygen carrier bed materials. The reactor had two connected pressure taps in order to measure the differential pressure in the bed and monitor the fluidization state. The flow rates of fluidizing gas were measured by mass flow controllers. The product gas from the reactor flowed through a cooler filled with $CaCl_2$ desiccant where the steam was condensed, and then was sent to the gas analyzers. Three gas analyzers were used to measure the gas composition simultaneously. The concentrations of CO_2, CO and SO_2 as well as the outlet gas flow rate were measured by a GA-21 Plus flue gas analyzer, the H_2 concentration was measured by an online GASboard-3100 coal gas analyzer, and the concentrations of CH_4, O_2 and H_2S were measured by Geotech Biogas Check. Note that the gas concentration in the paper refers to the gas volume fraction in the outlet gases.

Experimental Procedure

The experiments were performed in a laboratory-batched fluidized bed reactor under atmospheric pressure. Pure natural anhydrite or the mixture of natural anhydrite and lime were used as the oxygen carrier. In each run, 100 g of quartz sand with size range of 1500-2000 μm, served for preheating and distributing the reactant gas uniformly

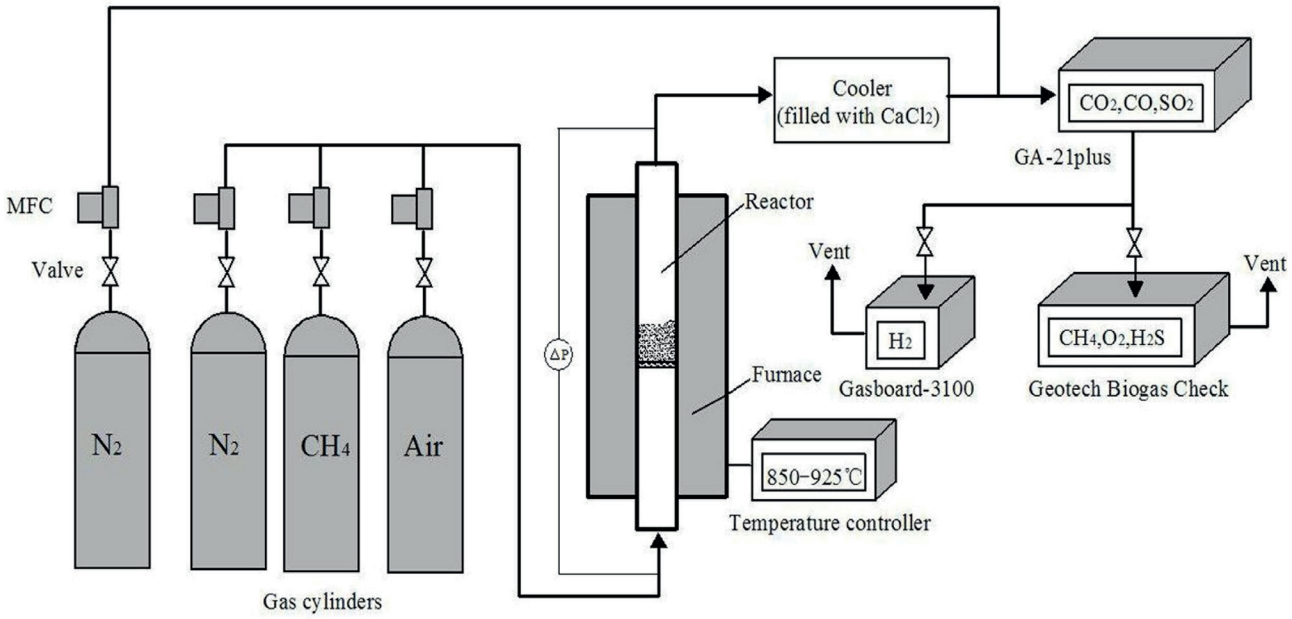

Figure 1. Schematic diagram of the experimental setup.

through the bed, was added above the porous plate. Then a new batch of 50 g of natural anhydrite as well as a certain amount of lime (0 g, 10 g, 20 g, 30 g, 40 g and 50 g) was placed on the quartz sand bed with the inside thermocouple located in the middle of the layer. During the preheating period, the reactor was purged with nitrogen gas flow. After the temperature reached the desired value (850, 900, 925 °C) and kept stable, the reduction gas of 25 vol.% CH_4 balanced by N_2, which was selected to avoid exceeding the terminal velocity of the particles due to the volume expansion of the reactant gas, was continuously introduced and the reduction time was 20 min. To avoid CH_4 and O_2 contact, nitrogen was introduced for a period of 5 min after the reducing period. After purging with N_2, the bed materials were exposed to the gas environment of 10 vol.% O_2 balanced by N_2 for the re-oxidation of the oxygen carrier. Then the fluidizing gas was switched to N_2 for the next cycling test. It should be noted that the oxidizing medium with lower O_2 concentration was used instead of air, which was to avoid the release of excess amounts of heat in the re-oxidation process.

When the test was finished, the system was again purged with nitrogen until the product gas was cleared away and the furnace was shut down. The sample was cooled in the environment of nitrogen to ambient temperature and was collected for further analysis. It should be noted that, as an inert gas, the N_2 was not considered in the results of this study. The experimental conditions are presented in Table 2.

Data Evaluation

The solid conversion of the oxygen carrier (X) is defined as:

$$X = \frac{m - m_{\text{red}}}{m_{\text{ox}} - m_{\text{red}}} \tag{1}$$

The conversion of the $CaSçO_4$ oxygen carrier as a function of time during the reduction period can be calculated based on the mass balance of oxygen from the $CaSO_4$ to the product gases, and the relationship is shown as below:

$$X_{\text{r,i}} = X_{\text{r,i-1}} - \int_{t_{i-1}}^{t_i} \frac{M_o n_{\text{out}}}{m_{\text{ox}} R_o} (4y_{\text{CO}_2,\text{out}} + 3y_{\text{CO,out}} - y_{\text{H}_2,\text{out}} + 2y_{\text{SO}_2,\text{out}}) dt \tag{2}$$

$$\frac{dX_{\text{i}}}{dt} = \frac{M_o n_{\text{out}}}{\text{m}_{\text{ox}} R_o} (4y_{\text{CO}_2,\text{out}} + 3y_{\text{CO,out}} - y_{\text{H}_2,\text{out}} + 2y_{\text{SO}_2,\text{out}}) \tag{3}$$

Similarly, the solid conversion during the oxidation period can be calculated as below:

$$X_{\mathrm{o,i}} = X_{\mathrm{o,i\text{-}1}} + \int_{t_{i-1}}^{t_i} \frac{2M_o}{m_{\mathrm{ox}} R_o} \left[(\dot{n}_{\mathrm{in}} y_{\mathrm{O_2,in}} - \dot{n}_{\mathrm{out}} (4y_{\mathrm{O_2,out}} + \frac{1}{2} y_{\mathrm{CO,out}} + y_{\mathrm{CO_2,out}} + y_{\mathrm{SO_2,out}}) \right] dt \tag{4}$$

$$\frac{dX_o}{dt} = \frac{2M_o}{m_{\mathrm{ox}} R_o} \left[(\dot{n}_{\mathrm{in}} y_{\mathrm{O_2,in}} - \dot{n}_{\mathrm{out}} (4y_{\mathrm{O_2,out}} + \frac{1}{2} y_{\mathrm{CO,out}} + y_{\mathrm{CO_2,out}} + y_{\mathrm{SO_2,out}}) \right] \tag{5}$$

Note that some of the oxygen in the air reactor was consumed by the deposited carbon, and some of the oxygen was released in the form of SO_2.

The sulfur release rate is defined as the ratio of moles of sulfur exiting the reactor on a dry basis to moles of sulfur-containing compound entering the reactor:

$$\chi_s = \int_{t_{i-1}}^{t_i} \frac{\dot{n}_{\mathrm{out}} (y_{\mathrm{SO_2,out}} + y_{\mathrm{H_2S,out}})}{n_{CaSO_4}} dt \times 100\% \tag{6}$$

The desulphurization rate can be defined through the sulfur release rate, and can be calculated as follows:

$$\eta_{\mathrm{s}} = \int_0^{t_i} \frac{n^{\mathrm{o}}_{\mathrm{out}} (y^o_{\mathrm{SO_2,out}} + y^o_{\mathrm{H_2S,out}}) - \dot{n}_{out} (y_{\mathrm{SO_2,out}} + y_{\mathrm{H_2S,out}})}{n^{\mathrm{o}}_{\mathrm{out}} (y^o_{\mathrm{SO_2,out}} + y^o_{\mathrm{H_2S,out}})} dt \times 100\% \tag{7}$$

An index S_I can be expressed as the relative intensity of the major peak of CaO divided by the relative intensity of the major peak of $CaSO_4$:

$$S_I = \frac{I_{\mathrm{CaO}}}{I_{\mathrm{CaSO_4}}} \tag{8}$$

The equilibrium constant of a chemical reaction (K_p) is the value of the reaction quotient when the reaction has reached equilibrium. For a general reaction aA(g) + bB(s) = pD(g) + qE(s), where A, B and D, E denote the reactants and products, respectively, and a, b, p and q refer to the stoichiometric number), it can be calculated as follows:

$$K_p = \frac{C_D^{\mathrm{p}}}{\mathrm{C_A^a}} = \frac{\mathrm{P_D^p}}{\mathrm{P_A^a}} \tag{9}$$

The standard Gibbs free energy of a reaction is related to the temperature, the ideal gas constant and the equilibrium of the specified reaction, and it can be expressed as:

$$\Delta \mathrm{G} = -RT \ln K_{\mathrm{p}} \tag{10}$$

RESULTS AND DISCUSSION

Desulphurization mechanism

Even though a great variety of reactants and products existed in these complex reactions, as illustrated in R1-R12, there were three kinds of solid matter, which were $CaSO_4$, CaS and CaO, respectively. Therefore, as one of the products in the side reactions, lime was added to $CaSO_4$ oxygen carrier in CLC of methane to achieve the desulphurization goal.

Thermodynamic analysis of the relevant reactions which illustrate the products distribution was discussed to investigate the desulphurization mechanism in this section. Figure 2 shows the equilibrium constants (K_p) of the $CaSO_4$ reduction reactions with lime addition as a function of temperature range from 600 °C to 1200 °C. The reduction of $CaSO_4$ to CaS (R1) was the main reduction reaction due to the larger equilibrium constant, and the reaction equilibrium would be shifted toward the

Table 2. Experimental condition.

Oxygen carrier	natural anhydrite with lime
Pressure (atm)	1
Reaction temperature (°C)	850, 900, 925, 950
Particle size (μm)	natural anhydrite: 180-250 lime: 125-180, 180-250, 250-350
Particle mass (g)	natural anhydrite: 50 lime: 10, 20, 30, 40, 50
Reduction gas	CH_4/N_2 = 25/75 %
Reduction gas flow (ml/min)	800
Reduction time (min)	20
Oxidation gas	O_2/N_2 = 10/90 %
Oxidation gas flow (ml/min)	1200
Oxidation time (min)	46
Diluent N_2 flow (ml/min)	400 (reduction) and 0 (oxidation)
Sweeping gas flow (ml/min)	1000

right side with the increase of temperature. Meanwhile, the equilibrium constants of the SO_2 or H_2S generation reactions (R3, R4, R5) also increased with temperature, which was consistent with the previous investigations (Song et al., 2008a,b; Zheng et al. 2010,2011). As a result, the temperature between 850 °C and 950 °C was chosen as the experimental temperature in the present work.

The lime particles changed the fluidization state in the fluidized bed so that the contact between the sulfur-containing gases and the CaO particles was improved, which means that the reaction rate would be enhanced. The standard Gibbs free energy of the reactions R8 and R9 was close to zero in the temperature range from 850 °C to 950 °C, indicating that the two reactions were reversible reactions and neither the forward nor the reversed reaction dominated. Therefore, the reactions R8 and R9 were more likely to be affected by the addition of the reactants or products, which was our starting point on sulfur-containing gases removal. The forward reactions corresponded to SO_2 or H_2S release (R3, R4) were dominant due to the CH_4-rich environment. However, after the lime addition, the reactions with smaller equilibrium constants (R8, R9) would go toward to the direction in which the sulfur-containing gases were consumed.

During the process of CaS oxidization, the standard Gibbs free energy of the relevant reactions was calculated over a wide range of temperatures, as shown in Figure 3. The standard Gibbs free energy of the reaction R2 was less than those of reactions R6 and R12 in the temperature range of 800-1000 °C, which demonstrated that the reaction R2 took precedence over reactions R6 and R12, and the main product of CaS oxidization was $CaSO_4$ rather than CaO. Similarly, the reaction direction of R9 was more probably influenced by the addition of lime because the Standard Gibbs free energy approximated to zero in the temperature range from 850 °C to 950 °C. As the residual CaO circulated to the air reactor, SO_2 released in the oxidization period could be removed through the forward reaction of R9. Based on the thermodynamic analysis, the idea of suppressing the sulfur-containing gases release by lime addition was feasible in the reduction and oxidization conditions, and the influence of the lime addition to $CaSO_4$ oxygen carrier was experimentally investigated in the next sections.

Effect of temperature

To evaluate the influence of lime addition on the solid conversion and sulfur capture efficiency of $CaSO_4$ oxygen carrier in CLC, experiments using natural anhydrite as the reference group were conducted at different temperatures of 850, 900, 925 and 950 °C. The added weight of lime was set to 10 g and the particle size was 180-250 μm. The concentrations of SO_2 and H_2S in the experiment at 950 °C exceeded the measuring range of the gas analyzers; thus, these results were not exhibited here.

Figure 4 shows the variation of the product gases concentrations on a dry basis as a function of time at 900 °C. During the reduction period, CO_2 and H_2O were produced by the reaction between $CaSO_4$ and parts of CH_4. It could be seen that the CO_2 concentration in the experiment of $CaSO_4$ with 10 g of lime addition was almost twice that without lime, which indicated that lime could improve the reactivity of $CaSO_4$ to CaS (R1). At the same time, a small part of CH_4 was partially oxidized to CO and H_2O, while another small part of CH_4 was decomposed into H_2 and carbon, and the carbon deposited on the particle surface. The concentrations of the by-product gases (i.e., H_2S, SO_2, H_2 and CO) moderately decreased with the addition of lime compared to that without lime addition, which demonstrated that the by-product gases release could be evidently suppressed by lime addition.

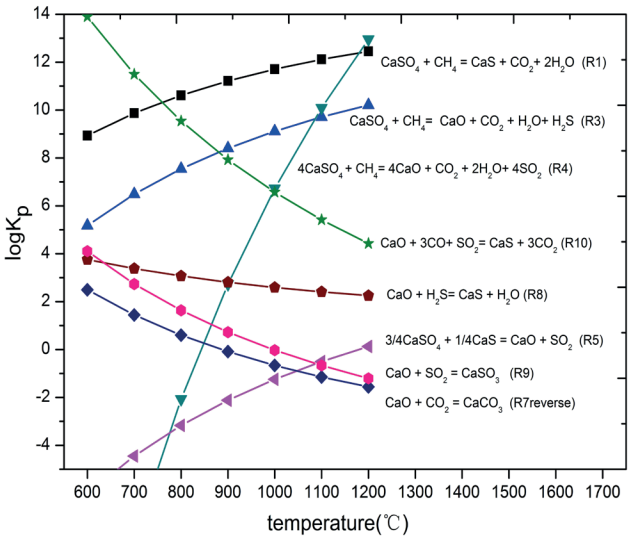

Figure 2. Equilibrium constants of relevant reactions in the reducing atmosphere

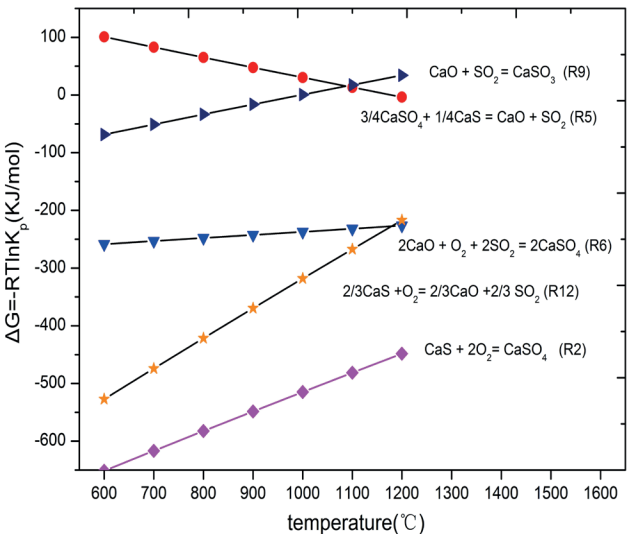

Figure 3. Standard Gibbs free energy of relevant reactions in the oxidizing atmosphere

Figure 4(b) and (d) show the variation of gas concentrations during the oxidation processes. Oxygen was not observed from the outlet during the early stage, which implied that the reaction rate at the initial time was so fast that a rapid conversion was obtained. Then the reaction rate gradually slowed down, and the O_2 concentration increased to 10 vol.% at the end of the oxidation period. That meant the conversion of CaS to $CaSO_4$ was completed at last, which could be proved by the XRD analysis. Note that little amount of CO_2 and SO_2 were observed at the beginning of the oxidation. The release of CO_2 can be explained as follows: some carbon was generated and then deposited on the surface of the particle in the reduction period, while in the oxidation period, this carbon would be oxidized by oxygen to produce CO_2. According to the literature, the SO_2 release could mainly be attributed to the side reactions R5 and R6 (Song et al., 2008b).

The effects of temperature and the lime addition on the conversion rate of $CaSO_4$ during the reduction/oxidation period are shown in Figure 5. It could be observed that the degree of reduction and oxidation increased with temperature, which was in agreement with some other investigations (Song et al., 2008a; Zheng et al., 2011). This result also indicated that the conversion rate of $CaSO_4$ increased with the temperature in the reduction period. Besides, the conversion rate of $CaSO_4$ in the experiment with lime addition was larger than that without lime addition. It should be noted that the conversion rate of $CaSO_4$ showed the same value in the oxidation period, because the reaction rate was controlled by the oxygen aeration rate (Su et al., 2016). The improvement of the conversion rate may be attributed to the catalysis of lime on the water-gas shift reaction (Teyssié et al., 2011). During the oxidation period, the oxygen carrier conversion could not be restored to the same level as before. As will be discussed later, this phenomenon resulted from the sulfur release during the reduction/oxidation process. Note that the conversion rate of $CaSO_4$ with lime addition at 900 °C was even slightly larger than that without lime at 925 °C. This could be attributed to the sulfidation reaction of lime,

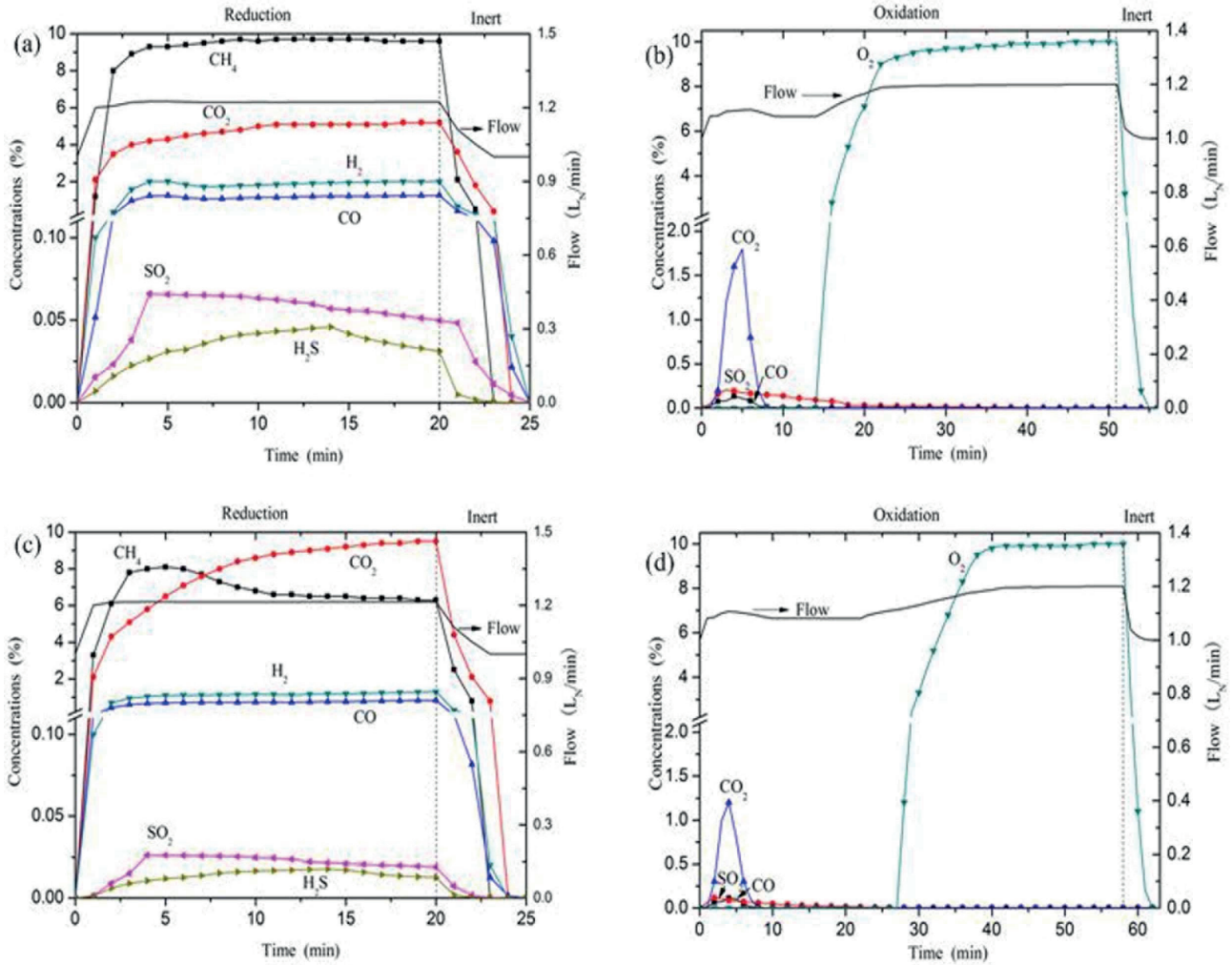

Figure 4. Product gas concentrations and dry gas flow during the first cycle: (a) and (b) $CaSO_4$ without lime, (c) and (d) $CaSO_4$ with lime. T = 900 °C, lime mass = 10 g, lime particle size = 180-250 μm. The dashed lines indicate the switch to an inert atmosphere.

which was favorable to the cyclic redox behavior of $CaSO_4$ oxygen carrier. Overall, the lime in the reactor could have a beneficial effect on the conversion of $CaSO_4$.

Figure 6 shows the sulfur release rate of the $CaSO_4$ oxygen carrier as a function of time during the first cycle. A positive correlation can be observed between the sulfur release rate and the temperature. As illustrated above, this may also be explained by the side reactions, including the competing reduction (R3, R4), solid-solid reaction (R5) and partial oxidation (R6). Satisfactorily, the sulfur release rate of $CaSO_4$ with lime addition was significantly lower than that without lime addition at the same temperature. And the desulphurization rates after the lime addition were up to 35.13%, 62.90% and 50.50% at 850, 900 and 925 °C, respectively. Based on the above analysis, the subsequent experimental temperature for $CaSO_4$ oxygen carrier with lime addition was set as 900 °C.

Effect of the calcium to sulfur ratio

The influence of the calcium to sulfur ratio (0.2, 0.4, 0.6, 0.8, 1.0, correspond to added weight of lime: 10g, 20g, 30g, 40g, 50g) on the performance of $CaSO_4$ and sulfur release was studied under the same particle size (180-250 μm) at 900 °C. The results are shown in Figure 7 and Figure 8, respectively. It can be seen from Figure 7 that the conversion rate of $CaSO_4$ increased with the calcium to sulfur ratio increasing in the reduction period. Interestingly, the conversion rate of $CaSO_4$ with 40 g of lime addition was very close to that with 50 g of lime addition. As shown in Figure 8, the lime addition resulted in the decrease of the sulfur release rate. Generally speaking, the more lime was added, the more the sulfur release decreased. The curves of the sulfur release rate had little differences between the calcium to sulfur ratios of 0.8 and 1.0 during the reduction period, while the sulfur release rate of $CaSO_4$ with 40 g lime addition was slightly lower than that with 50 g lime addition during the oxidation period. It was likely that the excess lime would cover the surface of CaS particles and reduce its contact with O_2, thus resulting in more sulfur release. The desulphurization rates of the various lime addition weights from 10 g to 50 g reached 62.90%, 67.98%, 76.28%, 81.67% and 80.97%, respectively. Considering the above results, 0.8 for the calcium to sulfur ratio was recommended in practical applications.

Effect of lime particle size

The lime particle size is a significant factor that influences the desulfurization rate in a traditional combustion system (Saastamoinen and Shimizu, 2007). In this section, the influence of lime particle size (range from 125 μm to 350 μm) on the desulfurization rate and the performance of $CaSO_4$ was investigated. The temperature was set to be 900 °C and the added weight of lime was 40 g.

The effect of lime particle size on the performance of the lime-promoted $CaSO_4$ oxygen carrier as a function of time at 900 °C is shown in Figure 9. The particle size of lime had little effect on the conversion of $CaSO_4$ oxygen carrier, in addition to a little difference in the final stage of oxidation, where the conversion of the oxygen carrier with larger lime particle size was slightly lower than that with the smaller one. In fact, it resulted from the sulfur release, which was illustrated in Figure 10. As shown in Figure 10, the decrease of the lime particle size resulted in the decrease of the sulfur release rate. Besides, it should be noted that the sulfur release rate of $CaSO_4$ with the lime particle size of 125-180 μm was approximately equal to that with 180-250 μm. Corresponding to the various particle size ranges of the lime (125-180 μm, 180-250μm, 250-350μm), the desulphurization rates were up to 79.38%, 80.97% and 81.56%, respectively. As mentioned in the literature (Saastamoinen and Shimizu, 2007; Yrjas

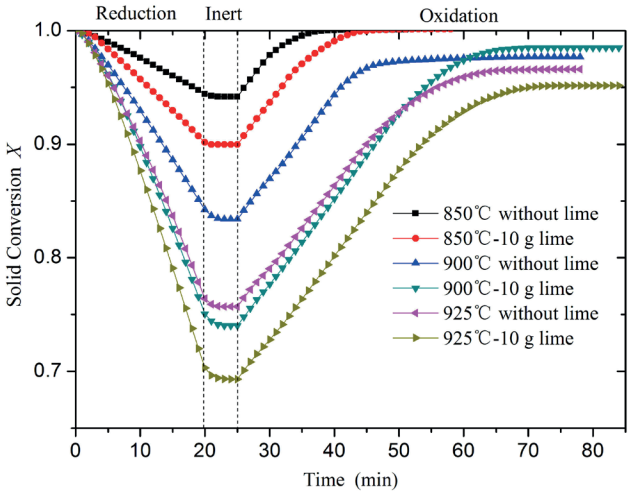

Figure 5. Oxygen carrier conversion (X) as a function of time in the temperature range of 850-925 °C.

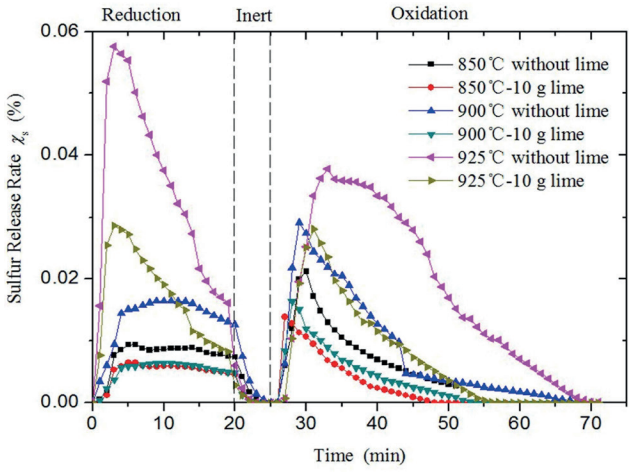

Figure 6. The sulfur release rate (X_s) of oxygen carrier as a function of time.

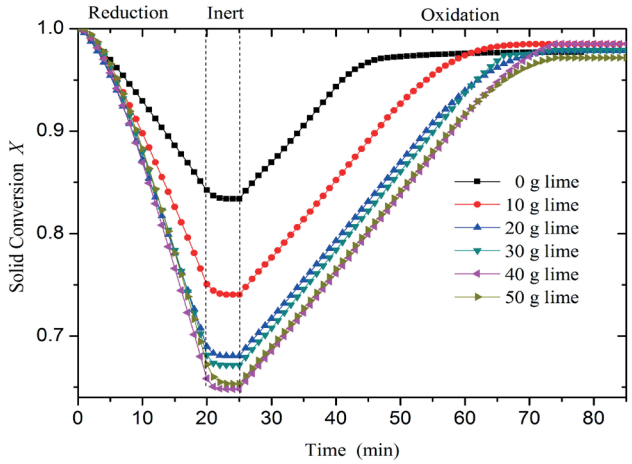

Figure 7. Oxygen carrier conversion (X) as a function of time at 900 °C with various masses of lime.

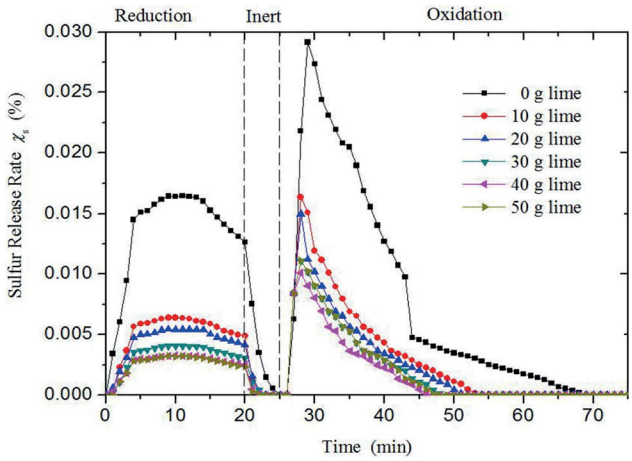

Figure 8. The sulfur release rate (X_s) of oxygen carrier as a function of time at 900 °C with various masses of lime.

et al., 1996), lime with smaller size had a higher reactivity. However, the small particles were more inclined to attrition and fragmentation, and the small particles could be carried out by the gas stream. Therefore, the 180-250 μm particle size of lime was recommended.

Multicycle test

In Figure 11(a), the outlet concentrations of CO_2, CO, CH_4 and O_2 are shown as a function of time. Most of the inlet CH_4 reacted with $CaSO_4$ to produce CO_2 and H_2O. The CO_2 concentration increased gradually in the first three reductions, and then decreased in the last two cycles. Meanwhile, the concentrations of CO and H_2 increased in the later stage of the fourth or fifth reduction process, which implied that the oxygen transfer capacity of $CaSO_4$ oxygen carrier decreased. Overall, it could be concluded that the reactivity of $CaSO_4$ increased for the initial cycles, but slightly decreased after three cycles. The above experiments illustrated that $CaSO_4$ oxygen carrier should not be reduced deeply in the reduction period. If the $CaSO_4$ oxygen carrier is reduced deeply, more CO and H_2 would be produced, instead of CO_2 and H_2O.

Figure 11(b) shows the variation of SO_2 and H_2S concentrations as a function of time during the cyclic test. It was clear that the H_2S and SO_2 concentrations were relatively stable during these five reduction reactions, but the SO_2 concentration increased during these five oxidation reactions, which may be due to the better adaptability of lime in the reduction process than in the oxidation process.

The conversion of oxygen carrier during the five cycles test is shown in Figure 12. It could be seen that the conversion of the oxygen carrier decreased gradually after reduction, which indicated that more oxygen in the oxygen carrier was utilized. The conversion could not restore the same level as before after oxidation, which could be ascribed to the release of sulfur. The majority of sulfur-containing gases were captured by the lime compared

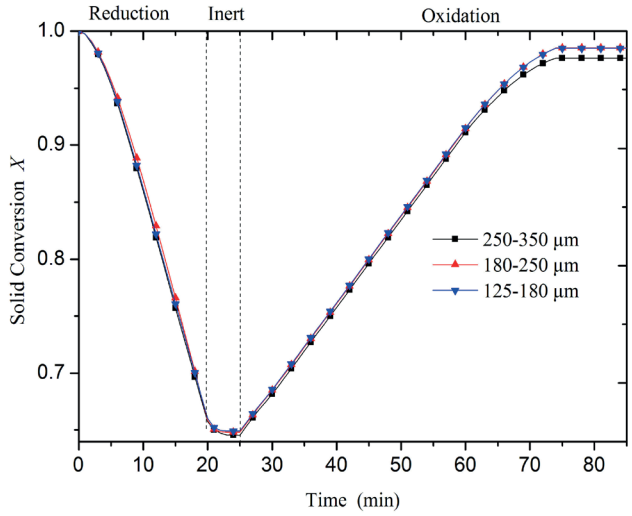

Figure 9. The effect of lime particle size on the conversion of CaSO4 as a function of time at 900 °C.

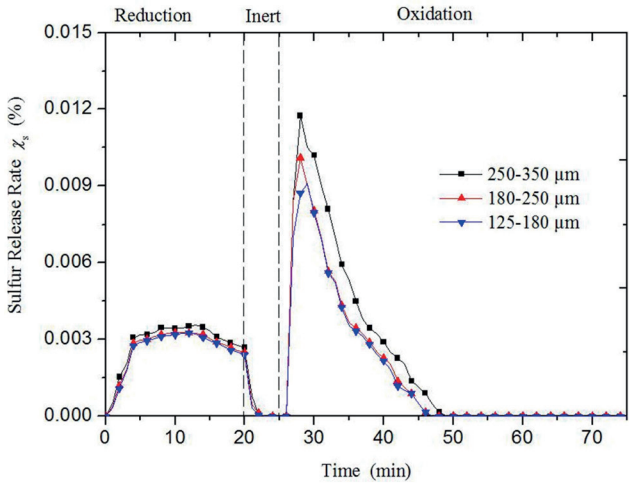

Figure 10. The effect of lime particle size on the sulfur release rate as a function of time at 900 °C.

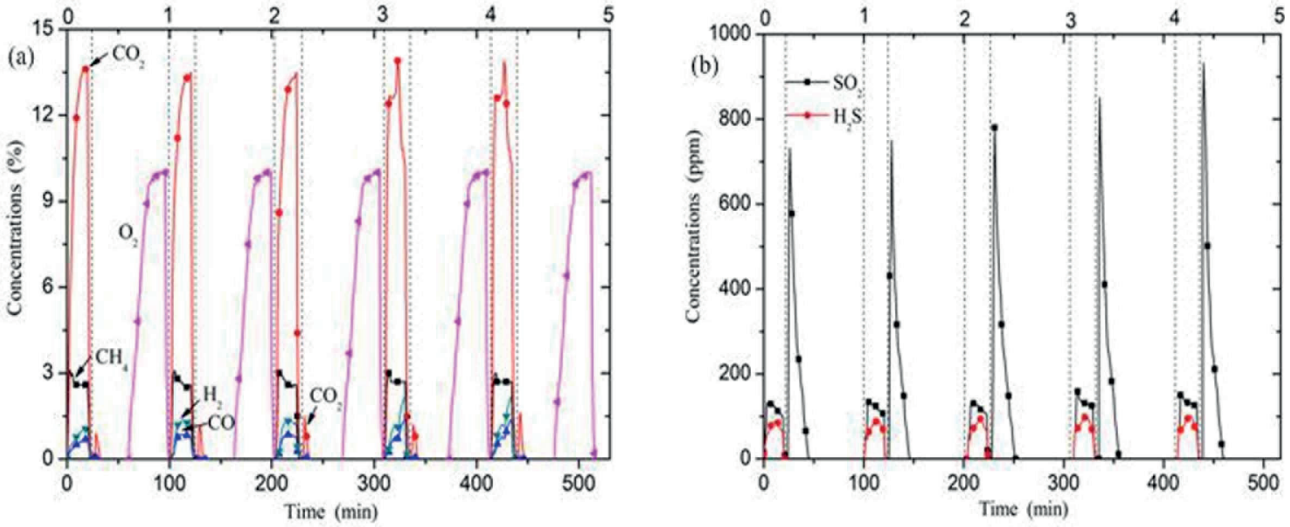

Figure 11. Products gas concentrations as a function of time during the five cycles: (a) outlet CO_2, CH_4, H_2, CO and O_2 concentrations, (b) outlet SO_2 and H_2S concentrations.

to the sulfur release of $CaSO_4$ oxygen carrier without lime addition (Song et al., 008b). However, the average desulphurization rate of lime was only 78.77% and the residual sulfur-containing gases would escape from the reactor, due to the limited contact between lime and the high-speed gas flow in the fluidized bed reactor. If the oxygen carrier particle made up of $CaSO_4$-core and pore-riched lime-shell was used, a better desulphurization rate could be achieved.

Characterization analysis

Phase characterization

The XRD patterns of the $CaSO_4$ oxygen carrier with and without lime addition are shown in Figure 13. It was evident that the main crystalline phase in the oxygen carrier was $CaSO_4$, as Figure 13(a) shows. Combined with the gas concentration analysis above, it could be concluded

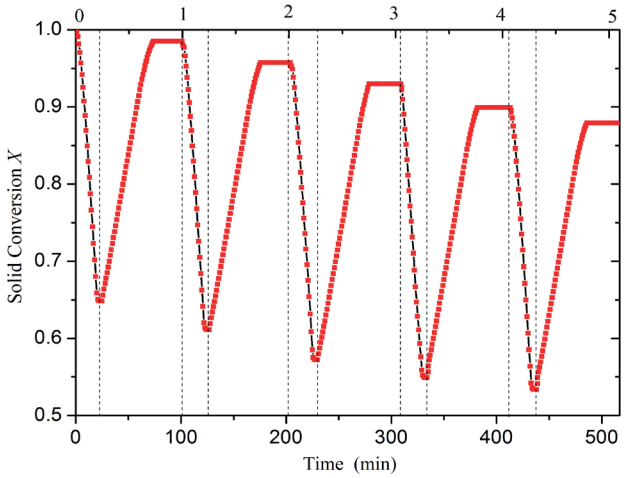

Figure 12. Variation of the oxygen carrier conversion as a function of time.

that most of $CaSO_4$ at 850 °C was not converted in the reduction period due to the low reactivity of $CaSO_4$. The index S_I, which meant the ratio of the relative intensity of the major peak for CaO phase to that for $CaSO_4$ phase, was introduced to express the relative content of CaO phase in the used oxygen carrier semi-quantitatively. The major peak of $CaSO_4$ phase was located at 2θ=25.52°, while the major peak of CaO phase was located at 2θ=37.35°. According to Figure 13, the index S_I and the relative standard deviation of S_I were calculated and presented in Table 3. The relative standard deviation of S_I could be used to evaluate the content of sulfur release or sulfur removal. The larger the relative standard deviation was, the more the sulfur was released from $CaSO_4$ oxygen carrier. It could be found from Table 3 that the sulfur release increased with temperature. Besides, the sulfur release decreased with the lime weight increase at the same temperature, which was consistent with the gas concentration analysis. The full-width half-maximum (FWHM) of the majorpeak could be used to represent the grain size of $CaSO_4$ in the used oxygen carrier. The FWHM of the sample (e) was 0.1574, while the value increased to 0.1771 after the 5th cycle, which suggested that the grain size of $CaSO_4$ decreased.

Surface morphology

Figure 14 shows the FESEM images of the surface morphology of the oxygen carrier particles after the oxidation. After the first cycle, the surface topography and the grain structures at 850 °C in Figure 14(a) were basically similar to that at 900 °C in Figure 14(b). However, as shown in Figure 14(c), a part of the grains on the external surface of the used oxygen carrier began sintering at 950 °C. The grain sintering on the external surface resulted from CaO formation (i.e., sulfur release) in the used oxygen carrier (Song et al., 2008b). So CaO formation

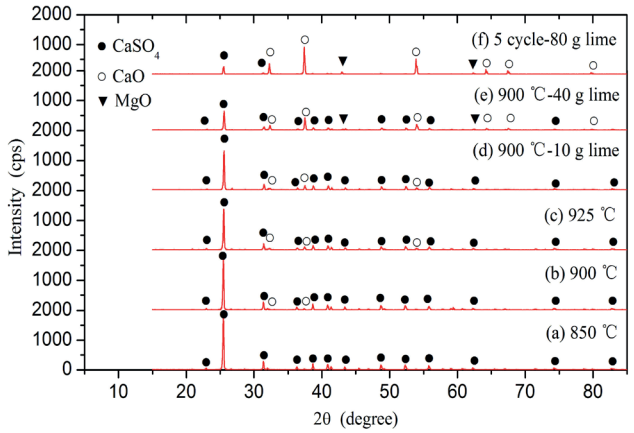

Figure 13. XRD patterns of a $CaSO_4$ oxygen carrier: (a) at 850 °C, (b) at 900 °C, (c) 925 °C, (d) at 900 °C with 10 g lime, (e) at 900 °C with 40 g lime and (f) at 900 °C after the 5th cycle oxidation.

Table 3. The index S_I and the relative standard deviation of S_I.

Sample	Index S_I	Theoretical index of S_I[a]	Relative standard deviation (%)
(a)	0.0138	0.0132	4.55
(b)	0.0271	0.0132	105.30
(c)	0.0820	0.0132	521.21
(d)	0.2014	0.1113	80.98
(e)	0.6573	0.5453	20.54
(f)	1.8160	1.6970	11.40

[a] The theoretical index of S_I comes from the refinement of the XRD spectrum according to the different mixing ratio of natural anhydrite and lime, and the content of CaO in natural anhydrite is also taken into account.

from $CaSO_4$ was unfavorable. When lime was added to $CaSO_4$, the surface of the samples became rougher and the size of grains dramatically declined, as shown in Figure 14(d-f). The change of surface morphology was beneficial to the diffusion of reactant gases into the core of oxygen carrier particles, thus facilitating the gas-solid reaction. Therefore, the addition of lime improved the performance of $CaSO_4$ oxygen carrier.

CONCLUSIONS

In this paper, CLC experiments of methane using $CaSO_4$ oxygen carrier with lime addition were carried out in a laboratory-batched fluidized bed reactor. The idea of removing sulfur-containing gases through lime addition was thermodynamically feasible in alternate oxidation and reduction processes. The effects of temperature, the calcium to sulfur ratio and lime particle size on $CaSO_4$ conversion and sulfur capture were investigated and a suitable operation condition was determined. Under the optimal condition, the multi-cycle test was conducted to evaluate the cyclic redox behavior.

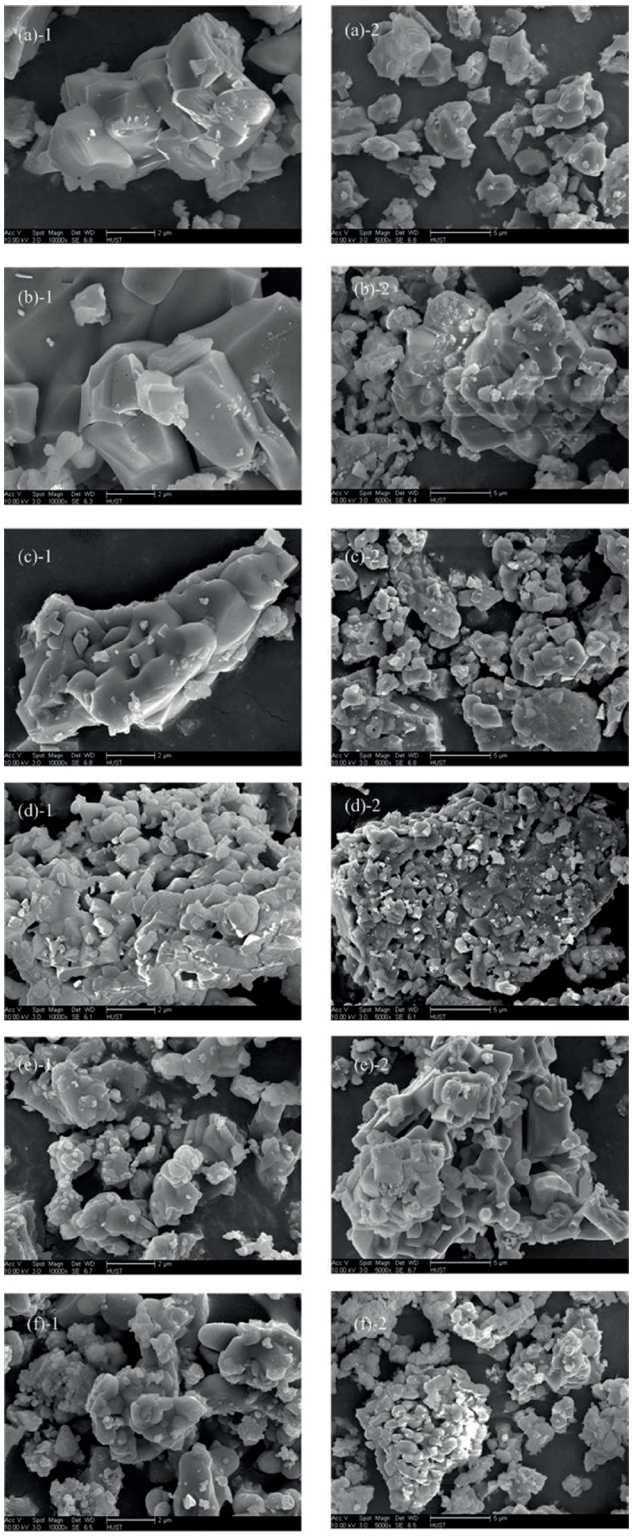

Figure 14. FESEM micrographs of a $CaSO_4$ oxygen carrier: (a) at 850 °C, (b) at 900 °C, (c) 925 °C, (d) at 900 °C with 10 g lime, (e) at 900 °C with 40 g lime and (f) at 900 °C after the 5th cycle of oxidation.

The addition of lime could improve the conversion rate of $CaSO_4$, which might be explained by the catalysis of lime on the water-gas shift reaction and the surface morphology change of the oxygen carrier after the lime addition. Both the reaction rate and the conversion of $CaSO_4$ were improved at high temperature. Besides, the sulfur-containing gases were captured by the lime additive. The analyses of the sulfur release and the XRD verified that the more lime was added, the higher the desulphurization rate achieved. The optimal operation condition was described as follows: 0.8 for the calcium to sulphur ratio, 180-250 μm for the particle size range of added lime and 900 °C for the operation temperature. The majority of sulfur-containing gases were captured during the cyclic test and the average desulphurization rate of lime was up to 78.77%.

NOMENCLATURES

C - the molar concentration of the reactant or product (mol/L)

I_{CaO} - relative intensity of the major peak of CaO in the XRD spectra of used oxygen carrier

I_{CaSO_4} - relative intensity of the major peak of $CaSO_4$ in the XRD spectra of used oxygen carrier

K_p - equilibrium constants of reactions

m - mass of oxygen carrier (kg)

m_{ox} - mass of the fully oxidized oxygen carrier (kg)

m_{red} - mass of the fully reduced oxygen carrier (kg)

M_o - atomic weight of oxygen (kg/mol)

$\dot{n}_{out}$ - molar flow of the gas exiting the reactor after condensation (mol/s)

n^0_{out} - molar flow of the gas exiting the reactor without lime after condensation (mol/s)

n_{CaSO_4} - molar of sulfur-containing compound entering the reactor (mol)

P - the pressure of the reactant gases or product gases (Pa)

R - constant of the ideal gases, 8.314 J $mol^{-1}K^{-1}$

R_o - oxygen ratio of the oxygen carrier, defined as

$$R_o = (m_{ox} - m_{red}) / m_{ox}$$

T - temperature(°C)

t - time (s)

$\frac{dX}{dt}$ - the reaction rate of oxygen carrier (1/s)

X_o - oxygen carrier conversion during the oxidation

X_r - oxygen carrier conversion during the reduction

$y_{i,out}$ - outlet mole fraction of the gas species i exiting the reactor after condensation

$y^0_{i,out}$ - outlet mole fraction of the gas species i exiting the reactor without lime after condensation

Greek letters

ΔH^0_{298K} - enthalpy change of the reaction under room temperature and atmospheric pressure (kJ/mol)

ΔG - standard Gibbs free energy of reactions (kJ/mol)

χ_s - sulfur release rate of oxygen carrier with lime (%)

χ^0_s - sulfur release rate of oxygen carrier without lime (%)

η_s - desulphurization rate of lime (%)

ACKNOWLEDGEMENTS

This work was supported by the National Natural Science Foundation of China (No.51406110), the Foundation for Outstanding Young Scientist in Shandong Province (No. BS2014NJ013) and the Youth Science Fund Project of Shandong Academy of Sciences (No. 2014QN014). The authors were also grateful to the analytical and testing centers of Shandong Province and Huazhong University of Science and Technology for XRD, FESEM-EDS and BET measurements.

REFERENCES

Abad, A., Mattisson, T., Lyngfelt, A. and Rydén M., Chemical-looping combustion in a 300 W continuously operating reactor system using a manganese-based oxygen carrier, Fuel, 85, 1174-1185 (2006).

Adánez, J., Dueso C., de Diego, L. F., García-Labiano, F., Gayán P. and Abad, A., Methane combustion in a 500 Wth chemical-looping combustion system using an impregnated Ni-based oxygen carrier, Energy & Fuels, 23, 130-142 (2009).

Andrus, H. E., Chiu, J. H., Thibeault, P. R. and Brautsch, A., Clean Coal and Fuel Systems, 34th International Technical Conference. Clearwater, Florida (2009).

Anthony, E. J. and Granatstein, D. L., Sulfation phenomena in fluidized bed combustion systems, Progress in Energy and Combustion Science, 27, 215-236 (2001).

Bragança, S. R., Jablonski, A. and Castellan, J. L., Desulfurization kinetics of coal combustion gases, Brazilian Journal of Chemical Engineering, 20, 161-169 (2003).

Bragança, S. R. and Castellan, J. L., FBC desulfurization process using coal with low sulfur content, high oxidizing conditions and metamorphic limestones, Brazilian Journal of Chemical Engineering, 26, 375-383 (2009).

Cao, Y. and Pan, W. P., Investigation of chemical looping combustion by solid fuels. 1. Process analysis, Energy & Fuels, 20, 1836-1844 (2006).

Cuadrat, A., Linderholm, C., Abad, A., Lyngfelt, A. and Adánez, J., Influence of limestone addition in a 10 kWth chemical-looping combustion unit operated with petcoke, Energy & Fuels, 25, 4818-4828 (2011).

de Diego, L. F., Ortiz, M., Adánez, J., García-Labiano, F., Abad, A. and Gayán, P., Synthesis gas generation by chemical-looping reforming in a batch fluidized bed reactor using Ni-based oxygen carriers, Chemical Engineering Journal, 144, 289-298 (2008).

Ding, N., Zhang C. W., Luo C., Zheng Y. and Liu Z. G., Effect of hematite addition to $CaSO_4$ oxygen carrier in chemical looping combustion of coal char, RSC Advances, 5, 56362-56376 (2015).

Ding, N., Wang, W. R., Zheng, Y., Luo, C., Fu, P. F. and Zheng, C. G., Development and testing of an interconnected fluidized-bed system for chemical looping combustion, Chemical Engineering & Technology, 35, 532-538 (2012).

Ding, N., Zheng, Y., Luo, C., Wu, Q. L., Fu, P. F. and Zheng, C. G., Development and performance of binder-supported $CaSO_4$ oxygen carriers for chemical looping combustion, Chemical Engineering Journal, 171, 1018-1026 (2011).

Doğu, T., The importance of pore structure and diffusion in the kinetics of gas-solid non-catalytic reactions: Reaction of calcined limestone with SO_2, Chemical Engineering Journal, 21, 213-222 (1981).

Hossain, M. M. and de Lasa. H. I., Chemical-looping combustion (CLC) for inherent CO_2 separations—a review, Chemical Engineering Science, 63, 4433-4451 (2008).

Johansson, M., Mattisson, T. and Lyngfelt, A., Creating a synergy effect by using mixed oxides of iron- and nickel oxides in the combustion of methane in a chemical-looping combustion reactor, Energy & Fuels, 20, 2399-2407 (2006).

Liu, H., Zailani, R. and Gibbs, B. M., Comparisons of pulverized coal combustion in air and in mixtures of O_2 /CO_2, Fuel, 84, 833-840 (2005).

Lyon, R. K. and Cole, J. A., Unmixed combustion: An alternative to fire, Combustion and Flame, 121, 249-261 (2000).

Mattisson, T. and Lyngfelt, A., The reaction between limestone and SO_2 under periodically changing oxidizing and reducing conditions-effect of temperature and limestone type, Thermochimica Acta, 325, 59-67 (1999).

Mattisson, T. and Lyngfelt, A., Reaction between sulfur dioxide and limestone under periodically changing oxidizing and reducing conditions-effect of cycle time, Energy & Fuels, 12, 905-912(1998).

Notz, R., Asprion, N., Clausen, I. and Hasse, H. Selection and pilot plant tests of new absorbents for post-combustion carbon dioxide capture. Chemical Engineering Research & Design, 85, 510-515 (2007).

Saastamoinen, J. J. and Shimizu, T., Attrition-enhanced sulfur capture by limestone particles in fluidized beds, Industrial & Engineering Chemistry Research, 46, 1079-1090 (2007).

Scott, S. A., Dennis, J. S., Hayhurst, A. N. and Brown, T., In situ gasification of a solid fuel andCO_2 separation using chemical looping, AIChE Journal, 52, 3325-3328 (2006).

Sebag, M. G., Bragança S. R., Normann. M. and Jablonski, A., The behavior of heavy metals in the process of desulfurization of Brazilian coal combustion gases by the addition of limestone, Brazilian Journal of Chemical Engineering, 18, 139-147 (2001).

Shen, L. H., Zheng, M., Xiao, J. and Xiao, R., A mechanistic investigation of a calcium-based oxygen carrier for chemical looping combustion, Combustion & Flame, 154, 489-506 (2008).

Song, Q. L., Xiao, R., Deng, Z. Y., Shen, L. H., Xiao, J. and Zhang, M. Y., Effect of temperature on reduction of $CaSO_4$ oxygen carrier in chemical-looping combustion of simulated coal gas in a fluidized bed reactor, Industrial & Engineering Chemistry Research, 47, 8148-8159 (2008a).

Song, Q. L., Xiao, R., Deng, Z. Y., Zheng, W. G., Shen, L. H. and Xiao, J., Multicycle study on chemical-looping combustion of simulated coal gas with a $CaSO_4$ oxygen carrier in a fluidized bed reactor, Energy &Fuels, 22, 3661-3672 (2008b).

Stern, M. C. and Hatton T. A., Bench-scale demonstration of CO_2 capture with electrochemically-mediated amine regeneration, RSC Advances, 4, 5906-5914 (2014).

Su, M., Ma, J., Tian, X., Zhao, H., Reduction Kinetics of Hematite as Oxygen Carrier in Chemical Looping Combustion, Fuel Processing Technology, DOI: 10.1016/j.fuproc.2016.05.015 (2016).

Tian, H. J., Guo, Q. J., Yue, X. H. and Liu, Y. Z., Investigation into sulfur release in reductive decomposition of calcium sulfate oxygen carrier by hydrogen and carbon monoxide, Fuel Processing Technology, 91, 1640-1649 (2010).

Teyssié, G., Leion, H., Schwebel, G. L., Lyngfelt, A. and Mattisson, T., Influence of lime addition to ilmenite in chemical-looping combustion with solid fuels, Energy & Fuels, 25, 3843-3853 (2011).

Xiao, R. and Song, Q. L., Characterization and kinetics of reduction of $CaSO_4$ with carbon monoxide for chemical-looping combustion, Combustion & Flame, 158, 2524-2539 (2011).

Yrjas, K. P., Zevenhoven, C. A. P. and Hupa, M. M., Hydrogen sulfide capture by limestone and dolomite at elevated pressure. 1. Sorbent performance, Industrial & Engineering Chemistry Research, 35, 176-183 (1996).

Zheng, M., Shen, L. H. and Xiao, J., Reduction of $CaSO_4$ oxygen carrier with coal in chemical-looping combustion: Effects of temperature and gasification intermediate, International Journal of Greenhouse Gas Control, 4, 716-728 (2010).

Zheng, M., Shen, L. H., Feng, X.Q. and Xiao, J., Kinetic model for parallel reactions of $CaSO_4$ with CO in chemical-looping combustion, Industrial & Engineering Chemistry Research, 50, 5414-5427 (2011).